DOI: 10.1002/cmdc.200800407

Synthesis and Conformational Analysis of Cyclotetrapeptide Mimetic β-Turn Templates and Validation as 3D Scaffolds

Luca Gentilucci,*[a] Giuliana Cardillo,[a] Alessandra Tolomelli,[a] Rossella De Marco,[a] Andrea Garelli,[a] Santi Spampinato,[b] Antonino Spartà,[b] and Eusebio Juaristi[c]

The initial event that is essential for modulating a biological response is molecular recognition between a ligand and a receptor. For peptide or protein ligands, recognition generally involves the interaction of restricted portions of the outer 3D surface with a complementary surface on the receptor. Peptide backbones generally serve as scaffolds for the key side chains that participate in the interaction. Very often, the backbones adopt secondary structure motifs, γ- or β-turns, or various kinds of helices. As a consequence, the bioactive compounds can, in principle, be substituted by smaller, simpler molecules that mimic the folded architectures.[1]

In particular, cyclic peptides have been widely used as templates for the design of turn-like structures.[1,2] However, small cyclic tetrapeptides[3] are difficult to synthesize, and they usually display mixtures of conformers due to *cis*/*trans* isomerization of peptide bonds. Conversely, larger cyclic penta- and hexapeptides are easier to prepare, but they retain significant backbone flexibility.[4]

Concerning peptidomimetic and nonpeptidic scaffolds,[1,2,5] several examples of cyclic, bicyclic, and spirocyclic compounds have been reported as turn-mimicking structures. Nevertheless, several cases have met with more limited success when the turn itself contains most of the pharmacophore elements.[1a,6] Therefore, cyclic peptides maintain their appeal as templates for applications in medicinal chemistry.

In the last few years, it has been reported that cyclic tetrapeptide structures enlarged by the introduction of a β-amino acid may render the structures easier to synthesize and conformationally more stable.[7] Very recently, we further customized a cyclotetrapeptide structure by implementation of a partially modified retro-inverso[8] (PMRI) sequence. A 1,2-diamine was used as β-amino acid analogue, and a malonic acid completed the sequence.[9] Conformational analysis revealed that the PMRI models containing an unsubstituted diamine exhibit notable flexibility. In contrast, the presence of a chiral, substituted 1,2-diamine (compound **1**, Figure 1) rendered the backbone more rigid, inducing β-turn structures and showing alternative conformations with respect to those of previously reported cyclotetrapeptide mimetics.[7]

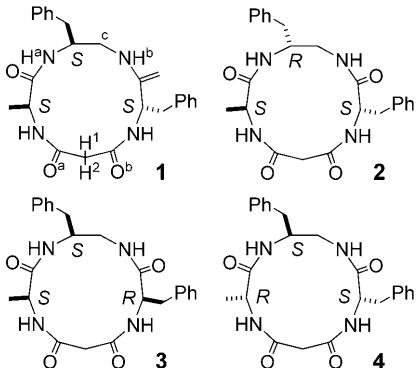

Figure 1. Structures of the partially modified retro-inverso cyclic tetrapeptide models **1**–**4**.

Herein we describe the syntheses and conformational analyses of all stereoisomers of PMRI cyclotetrapeptide models of the general sequence *cyclo*-[βPhe-ψ(NHCO)Ala-ψ(NHCO)Gly-Phe], obtained by introducing a chiral (*S*)- or (*R*)-1,2-diamine[10] as a β^2-amino acid mimetic, (*S*)- or (*R*)-phenylalanine, (*S*)- or (*R*)-alanine, and a malonyl residue (Figure 1). Furthermore, we provide preliminary validation of these compounds as effective scaffolds for the design of molecules with predictable 3D displays of the pharmacophores, useful for targeting specific bioactive conformations. As a prototypic example, we used those models for testing some selected novel RGD peptidomimetic compounds capable of interfering with integrin receptors.

We prepared models **1**–**4** as shown in Scheme 1, with the remaining being the enantiomers. The cyclic tetrapeptide analogues were prepared by solid-phase coupling of two dipeptide analogues **6** and **7**. Fragment **6** was prepared by a standard solution-phase procedure by coupling Fmoc-Phe-OH and Boc-protected diamine **5**,[10b,11] obtained, in turn, by reduction of Boc-PheNH$_2$ with BH$_3$.[12] The dipeptide was deprotected with dimethylamine (DMA), and the resulting crude product **6** was used without purification. Wang resin pre-loaded with alanine was treated with Meldrum's acid under microwave irradiation (MW) at 300 W. The complete conversion of resin-supported alanine to the dipeptide acid **7** was monitored by Kaiser's test. The solid-phase coupling of **7** with **6** afforded the tetrapeptide **8**. Subsequent cleavage from the resin with trifluoroacetic acid (TFA) and scavengers gave **9**, which was subjected to cyclization by treatment with diphenylphosphorylazide

[a] *Prof. L. Gentilucci, Prof. G. Cardillo, Dr. A. Tolomelli, Dr. R. De Marco, A. Garelli*
Department of Chemistry "G. Ciamician"
University of Bologna, via Selmi 2, 40126 Bologna (Italy)
Fax: (+39) 051 209 9456
E-mail: gentilucci@unibo.it

[b] *Prof. S. Spampinato, Dr. A. Spartà*
Department of Pharmacology
University of Bologna, via Irnerio 48, 40126 Bologna (Italy)

[c] *Prof. E. Juaristi*
CINVESTAV, National Polytechnic Institute
Av. Instituto Politecnico Nacional
2508 Col. San Pedro Zacatenco, 07360 (Mexico)

Supporting information for this article is available on the WWW under http://dx.doi.org/10.1002/cmdc.200800407.

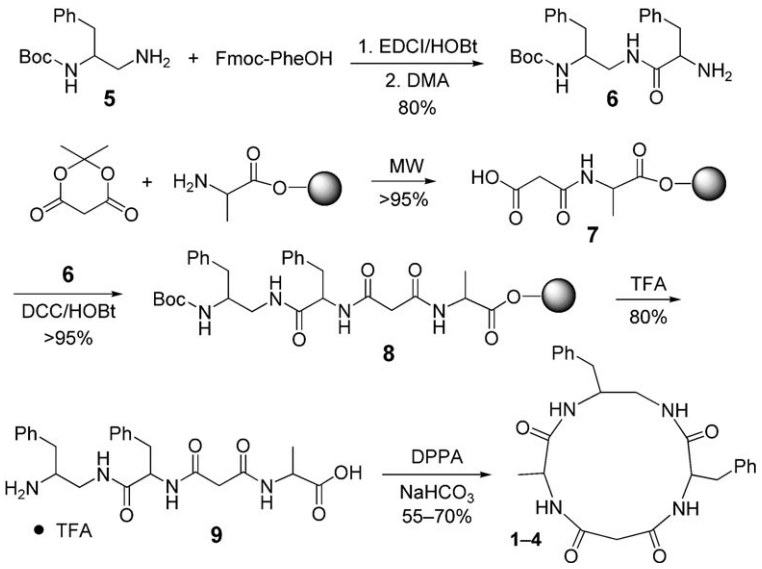

Scheme 1. Synthesis of partially modified retro-inverso cyclic models **1**–**4**.

(DPPA). After 48 h, the cyclic tetrapeptide analogues were isolated in 55–70% yield (cyclization step) by semipreparative RP-HPLC, and were 92–95% pure as determined by analytical RP-HPLC. The presence of stereoisomers originating from epimerization was excluded on the basis of HPLC–ESMS and ^{1}H NMR analyses.

The 3D structures of models **1**–**4** were investigated by NMR spectroscopy and molecular dynamics (MD) simulations. The NMR analysis was conducted using standard techniques at 400 MHz in the biomimetic medium [D_6]DMSO/H_2O 8:2;[13] (the compounds were nearly insoluble in water). For **1** and **3**, the analyses generally confirmed the results previously obtained in [D_6]DMSO,[9] with few differences. In any case, their conformational features are discussed herein for comparison.

For each peptide, ^{1}H NMR data revealed a single set of resonances, indicative of conformational homogeneity or a fast equilibrium.[4] COSY analysis allowed unambiguous assignment of the resonances. Variable temperature (VT)-^{1}H NMR experiments were used to deduce the presence of H bonds involving amide protons (Table 1).[14] For **1**, **3**, and **4**, the comparatively low $\Delta\delta/\Delta T$ values of diamine NH^a and NH^b (Figures 1, and 2) with respect to PheNH and AlaNH suggest the presence of secondary structures in equilibrium, alternatively stabilized by H bonds involving NH^a or NH^b, whereas for **2**, only the NH^b amide proton seems to be H bonded.

Table 1. $\Delta\delta/\Delta T$ values [ppb K^{-1}] of amide protons for **1**–**4** determined by VT-^{1}H NMR.[a]

Compd	PheNH	AlaNH	NH$^{a[b]}$	NH$^{b[b]}$
1	−5.0	−6.0	+1.2	−1.3
2	−6.0	−5.6	−4.5	−2.0
3	−3.5	−4.1	−1.3	−0.4
4	−3.9	−2.8	−0.75	−1.5

[a] Determined in [D_6]DMSO/H_2O (8:2) at 400 MHz over the range T = 298–338 K. [b] NH^a and NH^b, see Figures 1 and 2.

Molecular backbone conformations were investigated by 2D ROESY. The full list of ROESY cross-peaks is given in the Supporting Information (S.I.). The analyses indicated that the cyclic tetrapeptide analogues adopt all-*trans* conformations of the ω bonds, deduced from the absence of $H\alpha_i$–$H\alpha_{i+1}$ cross-peaks, indicative of *cis* peptide bonds. Structures consistent with the spectroscopic analyses were obtained by restrained MD, using the distances obtained from ROESY as constraints, and minimized with the AMBER[15] force field, with $\varepsilon = 4 \times r$. Simulations were conducted in vacuo by using a set of 50 random structures generated by an unrestrained high-temperature MD. The structures were subjected to restrained MD with a scaled force field, followed by a high-temperature simulation with full restraints. Finally, the system was gradually cooled, and the structures were minimized. The conformations with the lowest internal energy and the fewest number of violations of the experimental data were selected and analyzed (Figure 2 and S.I.).

The vast majority of the structures calculated for **1** and **2** by restrained MD did not show any violations of the restraints, and were well ordered. For **3** and **4**, on the other hand, the computations essentially gave two families of structures, **3a**/**3b** and **4a**/**4b** (Figure 2), with nearly the same energy, differing exclusively by the opposite orientation of PheNH, and AlaNH, respectively, each showing some constraint violations.

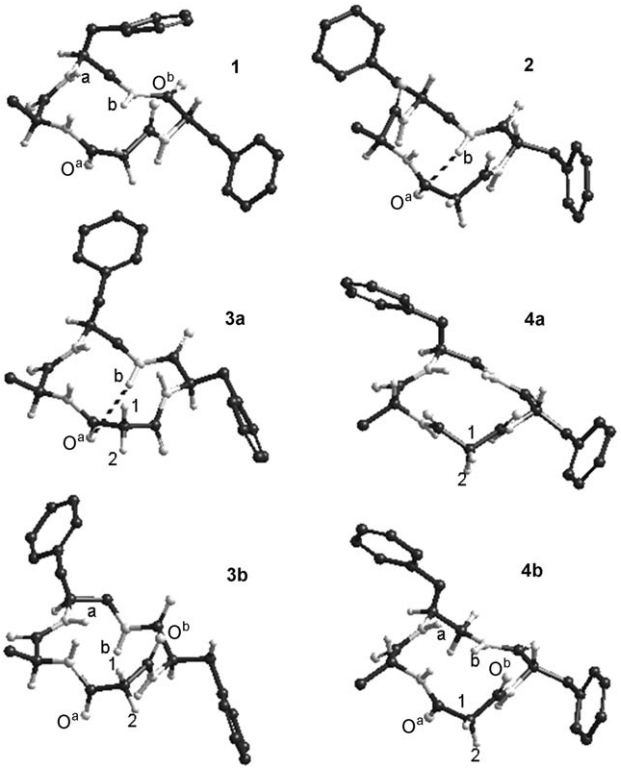

Figure 2. Representative lowest-energy structures of **1**–**4** calculated by ROESY-restrained MD with the fewest violations of ROESY data.

As expected, for **1** and **3**, the analyses confirmed the results previously obtained in [D_6]DMSO.[9]

To estimate the dynamic behavior of the cyclopeptides in water, and in particular to determine secondary structures stabilized by H bonds, the structures derived from ROESY were analyzed by unrestrained MD for 10 ns in a box of explicit, equilibrated water molecules. During the simulations, the structural features deduced by ROESY were maintained, and the examination of the trajectories revealed the occurrence of H bonds in agreement with VT-NMR analysis, not explicitly revealed by ROESY.

The representative structure of **1** calculated by ROESY-restrained MD in Figure 2 is compatible with a type I β-turn centered on Phe-diamine, and a second one centered on Ala-diamine. This structure shows no H bonds. However, analysis of the trajectories of the unrestrained MD revealed the presence of the two β-turn conformations in equilibrium, with NH^a and NH^b either alternately or simultaneously engaged in explicit H bonds with CO^b and CO^a, respectively (S.I.).

Concerning compound **2**, the ROESY-derived conformation shows a distinct H bond between NH^b and CO^a, as anticipated on the basis of VT-NMR, and an overall type II β-turn conformation on Ala-diamine (Figure 2). This conformation was very stable during the unrestrained MD simulation.

The occurrence of two slightly different structures for **3** and **4** reflects the observation of contradictory ROESY cross-peaks between H^1/H^2 protons and PheNH or AlaNH (Figure 2). In **3**, both AlaNH and PheNH show strong cross-peaks with H^1, and this situation is compatible with the structure **3a**. On the other hand, PheNH also gives a cross-peak of medium intensity with H^2. Moreover, while AlaNH gives a medium cross-peak with AlaHα, PheNH gives a strong cross-peak with PheHα. These observations are compatible with the structure **3b**, showing PheNH reversed relative to its position in **3a**. Both **3a** and **3b** are compatible with a type I β-turn on the Ala-diamine fragment, and **3a** manifests an explicit H bond between NH^b and CO^a. Compound **3b** is also compatible with a type I β-turn on Phe-diamine. The two structures **3a**/**3b** reasonably represent conformers in equilibrium. However, **3b** shows fewer distance violations and a structure more compatible with VT-NMR data, which are suggestive of two H bonds on both NH^a and NH^b. Unrestrained MD simulations performed on **3a** confirmed the stability of the H bonded structure. The unrestrained MD performed on **3b** show the H bonded structures involving NH^a and/or NH^b (S.I.). The simulations failed to reproduce the inversion of PheNH; evidently, this rotation is slow relative to the time selected for the simulation.

In a similar manner as with **3**, for compound **4** the strong cross-peaks between H^2 and both AlaNH and PheNH account for the structure **4a**, compatible with a type I β-turn centered on Phe-diamine. On the other hand, the cross-peak of medium intensity between AlaNH and H^1, and the strong cross-peak between AlaNH and AlaHα account for the structure **4b**, (Figure 2) characterized by a reversed orientation of AlaNH, compatible with a type I β-turn centered on Phe-diamine, and a second one on Ala-diamine. As for **3a**/**3b**, the two structures **4a**/**4b** likely represent conformers in equilibrium. During the unrestrained MD performed on **4a** and **4b**, analysis of the trajectories revealed the presence H bonded structures involving NH^a and NH^b (S.I.), as suggested by VT-NMR data.

In summary, compounds **1** and **2** show stable preferred backbone conformations, although **1** presents modest residual flexibility. The diastereomers **3** and **4** exhibit two slightly different conformers **a** and **b** in equilibrium; nevertheless, the overall 3D displays of the side chains are almost coincident. Notably, the different stereoisomers tend to adopt a similar 3D structure, with a β-turn centered on Ala-diamine and a second β-turn on Phe-diamine (with the exception of **2**), regardless of the stereochemistry assortment. This observation is not trivial; indeed, it is generally observed that the stereochemistry inversion of a distinct residue in a cyclic peptide leads to alternative secondary structures.[4, 8b, 16] This difference can be ascribed to the peculiar structure of the mimetics. Apparently, the PMRI cyclotetrapeptides show a strong tendency to stabilize type I or type II β-turn conformations involving the diamine amide protons.

It is accepted that the conformation of a cyclic peptide is scarcely controlled by the precise nature of the residues.[4, 8b] Therefore, the β-turn templates **1**–**4** and the respective enantiomers **5**–**8** can be used as topologically defined scaffolds for the design of biologically active compounds that having their pharmacophoric side chains in precise and well-defined diverse spatial arrangements. A schematic topographic depiction of the eight stereoisomeric PMRI cyclotetrapeptide models, simplified according to the Dunitz–Waser concept,[8b, 17] is shown in Figure 3. Relevant distances (in Å) between the Cβ atoms of the residues and H bonds are also shown.

To endorse the effectiveness of the novel PMRI scaffolds in medicinal chemistry, we used a selection of the models described above for the design of some unprecedented RGD peptidomimetic compounds capable of interfering with integrin receptors.[18] Integrins are a large family of heterodimeric transmembrane receptors involved in cell–cell adhesion and in the adhesion of cells to proteins of the extracellular matrix, such as fibronectin and vitronectin, as well as in signal transduction. Integrins are also involved in many major diseases, including cancer, asthma, thrombosis, osteoporosis, and risthenosis. Among the various kinds of integrins, $\alpha_v\beta_3$-integrins are generally considered privileged targets for anticancer therapy.

Many types of integrins, including $\alpha_v\beta_3$, bind their ligands by recognition of the same tripeptide motif: the Arg-Gly-Asp (RGD) sequence. As a consequence, many RGD-like ligands have been reported as $\alpha_v\beta_3$-integrin inhibitors. Massive SAR investigations of ligands based on peptide, peptidomimetic, or nonpeptide scaffolds have given detailed structural information about ligand–receptor interactions.[1d, 4a, 19] More recently, the crystal structure of the extracellular section of the receptor, with a cyclic RGD peptide bound to the active site, has been disclosed,[20] providing the opportunity to design novel antagonists based on the receptor-bound conformation of the RGD tripeptide.[21]

In essence, the criteria for designing effective $\alpha_v\beta_3$-integrin inhibitors reside in specific reciprocal orientations and distances between the Asp and Arg side chains, and in the orienta-

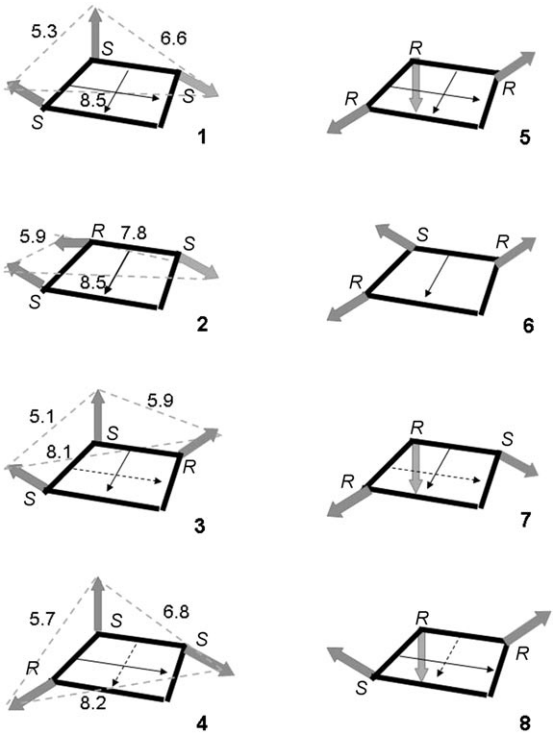

Figure 3. Schematic topographic depiction of the PMRI cyclotetrapeptide models **1**–**4** and the respective enantiomers **5**–**8**, with the distances (Å) between the Cβ atoms indicated. Large grey arrows show the pseudo-axial or pseudo-equatorial disposition of the side chains (Cα–Cβ vectors). Thin arrows indicate the H bonds.

tion of a third aromatic pharmacophore flanking Asp. Also, the presence of secondary structures in RGD ligands has often been correlated with specificity.[19,22] For this purpose, based on models **1**–**3** and **7**, we substituted Ala and Phe with Asp and Arg, respectively, to give the stereoisomeric cyclic PMRI RGD analogues **9**–**12** of general sequence *cyclo*-[βPhe-ψ-(NHCO)Asp-ψ(NHCO)Gly-Arg] (or *cyclo*-[βF-ψ(NHCO)D-ψ-(NHCO)GR] in brief; Table 2). For this preliminary investigation, models **1** and **2** were selected on the basis of their comparatively higher conformational stability, while models **3** and **7** were tentatively chosen for comparison.

We tested the activity of **9**–**12** as integrin antagonists by measuring the percent inhibition of fibronectin adhesion to the $\alpha_v\beta_3$-integrin-expressing cell line SK-MEL-24 (human malignant melanoma).[23] Fibronectin was immobilized on each well of a standard assay plate. Cells were pre-incubated with the cyclopeptides and dispensed on the wells. After removal of non-adherent cells, the number of adherent cells was quantified by fluorimetry. The activity of potential antagonists was determined by the number of adherent cells relative to the control. Table 2 shows the sequences of RGD mimetics **9**–**12**, the corresponding parent models **1**–**3**, and **7**, and the inhibitory activity (%) of **9**–**12**, at a concentration of 10^{-6} M, toward $\alpha_v\beta_3$-integrin-mediated cell adhesion. The activity of the well-known $\alpha_v\beta_3$-integrin antagonists Ac-DRGDS[23b] and GRGDNP,[24] assayed under the same conditions, was also measured as a positive control. For the inhibitory activity at various ligand concentrations, see the S.I.

Statistical analysis reveals that all the compounds display significant and concentration-dependent potency in blocking SK-MEL-24 cell adhesion (S.I.). The biological activities of the four peptides vary radically (**10** > **11** > **12** ≈ **9**), although the constitution of the peptides is identical. This observation confirms the anticipation that compounds based on the PMRI cyclotetrapeptide models behave as topologically distinct structures. These results can be tentatively rationalized by comparing the topographic depiction of the parent models **1**–**3** and **7** (Figure 3) with the structural requisites reported for $\alpha_v\beta_3$-integrin inhibitors (the conformations of **9**–**12** have not been reexamined[25]). An illustrative model of the bioactive conformation of a prototypic $\alpha_v\beta_3$-selective cyclopentapeptide ligand[19a,26] is shown in Figure 4A.[20,21] The simplified Dunitz–Waser sketch, Figure 4B and the relevant distances between the pharmacophoric groups and between the Cβ atoms are also presented.

For the noteworthy conformational freedom of the side chains, the precise disposition of the pharmacophoric groups of a cyclopeptide in solution and in the bioactive conformation can be very different. For this reason, the 3D structure of a cyclopeptide is often characterized by the disposition of the Cβ atoms with respect to the cyclopeptide scaffold.[4a,8b,16,19a] Therefore, the use of topographic models, such as those depicted in Figures 3 and 4B, can be very useful to compare the structures of different compounds.

Compound **10** shows the best activity as an inhibitor of integrin-mediated adhesion; it is inferior, but still comparable to that of the reference compound Ac-DRGD (Table 2). It can be perceived that **10** (see model **2**, Figure 3) shows a comparatively higher topological similarity with the prototypic pharmacophore (Figure 4B) in comparison with the other compounds (see models), both in terms of the orientations and distances between the Cβ atoms. The lower activities displayed by **11** and **12** seem to be correlated with a short distance between the Cβ atoms of Asp and Arg, and the diamine (models **3** and **7**, Figure 3). Interestingly, compound **9** shows the lowest inhibitory activity, despite having

Table 2. Inhibition of $\alpha_v\beta_3$-integrin-mediated SK-MEL-24 cell adhesion of fibronectin in the presence of **9**–**12**, Ac-DRGDS, and GRGDNP.

Ligand	Structure	Model	Inhibition [%][a]
9	*cyclo*-[(*S*)-βF-ψ(NHCO)D-ψ(NHCO)GR]	**1**	32 ± 3
10	*cyclo*-[(*R*)-βF-ψ(NHCO)D-ψ(NHCO)GR]	**2**	55 ± 2
11	*cyclo*-[(*S*)-βF-ψ(NHCO)D-ψ(NHCO)G-(*R*)-R]	**3**	43 ± 1
12	*cyclo*-[(*S*)-βF-ψ(NHCO)-(*R*)-D-ψ(NHCO)GR]	**7**	35 ± 2
–	Ac-DRGDS	–	69 ± 1
–	GRGDNP	–	40 ± 3

[a] Determined at a compound concentration of 10^{-6} M; values represent the mean ± SEM of three experiments.

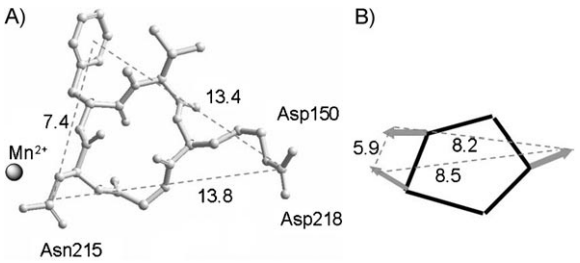

Figure 4. Models of the bioactive conformation of the $\alpha_v\beta_3$-selective ligand *cyclo*-[RGDf(NMe)V], along with A) the distances (Å) between the pharmacophores, and B) between the Cβ atoms of Asp, D-Phe, and Arg.

a similar disposition of Asp and Arg side chains with respect to **10** (based on the comparison of the parent models **1** and **2**), highlighting the role of the aromatic pharmacophoric group of the diamine.

In conclusion, we have presented cyclotetrapeptide mimetic β-turn templates based on the retro-inverso concept, and we have described their conformational and topological features. The 3D structures are largely dominated by the tendency of the diamine residue to stabilize β-turn structures. As a consequence, the various stereoisomers can be viewed as diverse scaffolds assembled on a common β-turn template, which can find applications in medicinal chemistry. To confirm the assumptions, we prepared a selected set of RGD peptidomimetics based on the structures of the scaffold models. The biological assay gave evidence for a clear relationship between the supposed 3D structures of the RGD mimetics and the experimental activities as inhibitors of integrin-mediated cell adhesion.

Experimental Section

General methods. Unless stated otherwise, standard chemicals were obtained from commercial sources and used without further purification. Analytical RP-HPLC was performed with an ODS column (4.6 μm particle size, 100 Å pore diameter, 250 mm, DAD 210 nm) using a linear gradient of H_2O/CH_3CN (9:1→2:8) over 20 min at a flow rate of 1.0 mL min^{-1}, followed by 10 min isocratic H_2O/CH_3CN 2:8. Chiral HPLC analysis was performed on a Chiralcel ODH column [0.46 cm (∅) × 25 cm (*l*)], *n*-hexane/2-propanol 85:15, at 0.8 mL min^{-1}. Semipreparative RP-HPLC was performed on a C_{18} column (7 μm particle size, 21.2×150 mm) with a linear gradient of H_2O/CH_3CN (7:3→100% CH_3CN) over 15 min, at a flow rate of 12 mL min^{-1}. Fluorimetry to evaluate the number of adherent cells was performed with a Victor2 multilabel counter. ^{1}H NMR spectra were recorded at 400 MHz at room temperature with 5-mm tubes, using 0.01 M peptide. Chemical shifts (δ) are reported relative to the solvent peak. VT-^{1}H NMR experiments were performed over the range T=298–348 K; 2D spectra were acquired in the phase-sensitive mode and processed using a 90° shifted, squared sine-bell apodization. ^{1}H NMR resonances were assigned from 2D gCOSY and 2D ROESY spectra; gCOSY experiments were recorded with a proton spectral width of 3103 Hz. ROESY experiments were recorded with a mixing time of 300 or 350 ms with a proton spectral width of 3088 Hz. Materials for bioassays were purchased from Invitrogen (Carlsbad, CA, USA) and Cambrex (Walkersville, MD, USA). SK-MEL-24 (human malignant melanoma) cells were obtained from American Type Culture Collection (ATCC, Rockville, MD, USA). Plates (96-well) were obtained from Corning, New York, NY, USA. The Victor2 multilabel counter was obtained from PerkinElmer (Waltham, MA, USA).

Synthesis of 6. HOBt (0.12 g, 0.9 mmol) was added to a stirred solution of Fmoc-Phe-OH (0.29 g, 0.75 mmol) in 9/1 CH_2Cl_2/DMF (9:1, 10 mL) at room temperature. After 10 min, **5**[10b,11] (0.19 g, 0.75 mmol, 94% pure by chiral HPLC analysis, see *General methods*), EDCI·HCl salt (0.19 g, 0.9 mmol) and TEA (0.15 mL, 1.1 mmol) were added while stirring at room temperature. After 3 h, the mixture was diluted with CH_2Cl_2, and the solution was washed with 0.5 M HCl, and saturated Na_2CO_3. The organic layer was dried over Na_2SO_4, and the solvent was removed at reduced pressure. The protected dipeptide was isolated by crystallization from CH_2Cl_2/Et_2O (0.39 g, 83%, 85% pure by RP-HPLC). ESMS *m/z*: 620.3 [*M*+1]; calcd: 620.3. The crude protected dipeptide was treated while under magnetic stirring with 2 M DMA in THF (5 mL) at room temperature. After 30 min, the solution was evaporated at reduced pressure, and the treatment was repeated. The residue was triturated in *n*-hexane. The dipeptide **6** (0.23 g, 96%, 82% pure by RP-HPLC) was used without further purification. ESMS *m/z*: 398.3 [*M*+1], calcd: 398.2.

Synthesis of 9. Wang resin pre-loaded with alanine (0.5 g, 0.6 (mmol Ala) g^{-1}) was suspended in DMF (4 mL) and treated with Meldrum's acid (0.36 g, 2.4 mmol). The suspension was heated by MW irradiation at 300 W. After 90 min, the resin was filtered and washed with MeOH, DMF, and CH_2Cl_2 (5 mL each), and the procedure was repeated twice. The complete conversion of resin-supported Ala to the resin-bound dipeptide acid **7** was monitored by Kaiser's test.

The resin-bound dipeptide **7** was suspended in CH_2Cl_2 (5 mL) and treated with **6** (0.24 g, 0.6 mmol), DCC (0.13 g, 0.7 mmol), and HOBt (0.10 g, 0.8 mmol). The mixture was mechanically shaken for 6 h. The mixture was then filtered, and the resin was washed with MeOH, DMF, and CH_2Cl_2 (5 mL each). The washing procedure was repeated twice.

Peptide cleavage. The resulting resin-bound **8** was suspended in a mixture of TFA (5 mL), H_2O (0.15 mL), TIPS (0.1 mL), and PhOH (0.15 g), and mechanically shaken at room temperature. After 2 h, the mixture was filtered, the resin was washed twice with 10% TFA in Et_2O (5 mL), and twice with Et_2O. The collected filtrates were evaporated, and the residue was precipitated from ice-cold Et_2O. The resulting precipitate was centrifuged at 4000 rpm (ALC Centrifugette 4206), and the crude solid peptide·TFA salt **9** was crystallized from MeOH/Et_2O (0.14 g, 80%, 82% pure by RP-HPLC). ESMS *m/z*: 455.3 [*M*+1]; calcd: 455.2.

Cyclization to 1–4. The peptide·TFA salt **9** (0.14 g, 0.24 mmol) was dissolved in dry DMF (60 mL) and treated, while under magnetic stirring, with $NaHCO_3$ (0.25 g, 3 mmol) and DPPA (0.17 g, 0.6 mmol) at room temperature. After 72 h, the mixture was filtered, and the solvent was distilled at reduced pressure. The residue was diluted with H_2O (5 mL), and the mixture was extracted with EtOAc (4× 20 mL). The collected organic layers were dried over Na_2SO_4, and the solvent was evaporated at reduced pressure. The oily residue was purified by semipreparative RP-HPLC to afford the cyclopeptides **1**–**4** (0.58–0.73 g, 55–70% yield, 92–95% pure by RP-HPLC). ESMS *m/z*: 437.3 [*M*+1]; calcd: 437.2.

Conformational analysis. The restrained MD simulations were conducted using the AMBER[15] force field with a distance-dependent $\varepsilon = 4 \times r$. A 100-ps simulation at 1200 K was used for generating 50

random structures that were subsequently subjected to a 20-ps restrained MD with a 50% scaled force field at the same temperature, followed by 20 ps with full restraints (distance force constant: 7 kcal mol^{-1} Å^2), after which the system was cooled over 10 ps to 50 K. Due to the absence of Hα_i and Hα_{i+1} ROESY cross-peaks, the ω bonds were set at 180° (force constant: 16 kcal mol^{-1} Å^2). Only ROESY-derived constraints were included in the restrained MD. H bond interactions as well as torsion angle restraints were excluded. ROESY intensities were classified as very strong, strong, medium, and weak, and were associated with distances of 2.3, 2.6, 3.0, and 4.0 Å, respectively. Geminal couplings and other clear correlations were discarded. The resulting structures were minimized with 3000 cycles of steepest descent and 3000 cycles of conjugated gradient (convergence: 0.01 kcal Å^{-1} mol^{-1}). The structures that showed the lowest internal energy and the fewest violations of the experimental data were selected and analyzed. MD simulation in explicit water was performed for 10.0 ns at 298 K using the AMBER force field in a 30×30×30 Å^3 box of standard TIP3P models of equilibrated water,[27] with a minimum solvent–solute distance of 2.3 Å, at constant temperature and pressure (Berendsen scheme,[28] bath relaxation constant: 0.2).

Cell adhesion assays. SK-MEL-24 cells were routinely grown in minimal essential medium (MEM) supplemented with 10% fetal bovine serum, nonessential amino acids, and sodium pyruvate. Cells were kept at 37 °C in a 5% CO_2 humidified atmosphere. Plates (96-well) were coated by passive adsorption with fibronectin (10 μg mL^{-1}) overnight at 4 °C. Cells were counted and exposed to the drug at three different concentrations (10^{-8}, 10^{-6}, and 10^{-4} M) for 30 min at room temperature to allow ligand–receptor equilibrium. Stock solutions (10^{-2} M) of the assayed compounds were prepared in 33% DMSO and 66% phosphate-buffered saline (PBS) (*v*/*v*), and were further diluted with PBS alone. Control cells were exposed to the same concentration of DMSO (vehicle). At the end of the incubation time, the cells were plated (50000 cells per well) and incubated at room temperature for 1 h. All the wells were then washed with PBS to remove the nonadherent cells, and the hexosaminidase substrate, 4-nitrophenyl-*N*-acetyl-β-D-glucosaminide (50 μL, dissolved at 7.5 mM in 0.09 M citrate buffer solution, pH 5, and mixed with an equal volume of 0.5% Triton X-100 in H_2O), was added. This product is a chromogenic substrate for β-*N*-acetylglucosaminidase that is transformed in 4-nitrophenol, the absorbance of which is measured at $\lambda = 405$ nm. As previously described,[29] there is a linear correlation between absorbance and enzymatic activity. It is therefore possible to identify the number of adherent cells in treated wells, interpolating the absorbance values of the unknowns in a calibration curve. The reaction was blocked by adding 100 μL stop solution (50 μM glycine, 5 μM EDTA, pH 10.4), and the plate was read in a multilabel counter. Experiments were carried out in triplicate. All data are expressed as the mean ± SEM for the number of experiments indicated. Statistical comparisons were made by ANOVA and post hoc Dunnet's or Turkey's tests with differences of $p < 0.05$ considered significant. Data were analyzed using Prism 5.0 software (GraphPad Software Inc., San Diego, CA, USA).

Acknowledgements

We thank MIUR (PRIN 2006) and MAE (Bilateral Project Italia–Mexico) for financial support (Con il contributo del Ministero degli Affari esteri, Dir. Generale per la Promozione e la Cooperaz. Culturale), Stepbio Peptide Chemistry Discovery Division (http://www.stepbio.it), and Mr. Cathal Daly (on leave from Trinity College, Dublin, Ireland) for collaboration.

Keywords: β-turns · conformational analysis · cyclopeptides · integrin receptors · peptide mimetics

[1] a) V. J. Hruby, P. M. Balse, *Curr. Med. Chem.* **2000**, *7*, 945–970; b) J. D. A. Tyndall, B. Pfeiffer, G. Abbenante, D. P. Fairlie, *Chem. Rev.* **2005**, *105*, 793–826; c) V. J. Hruby, R. S. Agnes, *Biopolymers* **1999**, *51*, 391–410; d) L. Gentilucci, A. Tolomelli, F. Squassabia, *Curr. Med. Chem.* **2006**, *13*, 2449–2466.

[2] M. MacDonald, J. Aubé, *Curr. Org. Chem.* **2001**, *5*, 417–438.

[3] a) N. Loiseau, J.-M. Gomis, J. Santolini, M. Delaforge, F. Andre, *Biopolymers* **2003**, *69*, 363–385; b) P. Mora, C. Mas-Moruno, S. Tamborero, L. J. Cruz, E. Perez-Paya, F. Albericio, *J. Pept. Sci.* **2006**, *12*, 491–496.

[4] a) H. Kessler, *Angew. Chem.* **1982**, *94*, 703–703; *Angew. Chem. Int. Ed. Engl.* **1982**, *21*, 512–523; b) S. J. Stradley, J. Rizo, M. D. Bruch, A. N. Stroup, L. M. Gierasch, *Biopolymers* **1990**, *29*, 263–287; c) X. M. Zhang, G. V. Nikiforovich, G. R. Marshall, *J. Med. Chem.* **2007**, *50*, 2921–2925.

[5] G. Schneider, P. Schneider, S. Renner, *QSAR Comb. Sci.* **2006**, *25*, 1162–1171.

[6] a) A. Giannis, T. Kolter, *Angew. Chem.* **1993**, *105*, 1303–1326; *Angew. Chem. Int. Ed. Engl.* **1993**, *32*, 1244–1267; b) J. Gante, *Angew. Chem.* **1994**, *106*, 1780–1802; *Angew. Chem. Int. Ed. Engl.* **1994**, *33*, 1699–1720.

[7] a) F. Schumann, A. Muller, M. Koksch, G. Muller, N. Sewald, *J. Am. Chem. Soc.* **2000**, *122*, 12009–12010; b) M. P. Glenn, M. J. Kelso, J. D. A. Tyndall, D. P. Fairlie, *J. Am. Chem. Soc.* **2003**, *125*, 640–641; c) A. S. Norgren, F. Buttner, S. Prabpai, P. Kongsaeree, P. I. Arvidsson, *J. Org. Chem.* **2006**, *71*, 6814–6821; d) N. Maulucci, M. G. Chini, S. Di Micco, I. Izzo, E. Cafaro, A. Russo, P. Gallinari, C. Paolini, M. C. Nardi, A. Casapullo, R. Riccio, G. Bifulco, F. De Riccardis, *J. Am. Chem. Soc.* **2007**, *129*, 3007–3012.

[8] a) M. Chorev, M. Goodman, *Acc. Chem. Res.* **1993**, *26*, 266–273; b) J. Wermuth, S. L. Goodman, A. Jonczyk, H. Kessler, *J. Am. Chem. Soc.* **1997**, *119*, 1328–1335; c) M. D. Fletcher, M. M. Campbell, *Chem. Rev.* **1998**, *98*, 763–795; d) K.-J. Kim, S.-W. Park, S. S. Yoon, *J. Kor. Chem. Soc.* **2000**, *44*, 286–289; e) Y. Han, C. Giragossian, D. F. Mierke, M. Chorev, *J. Org. Chem.* **2002**, *67*, 5085–5097; f) H. Tamamura, M. Mizumoto, K. Hiramatsu, S. Kusano, S. Terakubo, N. Yamamoto, J. O. Trent, Z. Wang, S. C. Peiper, H. Nakashima, A. Otaka, N. Fujii, *Org. Biomol. Chem.* **2004**, *2*, 1255–1257; g) M. Chorev, *Biopolymers* **2005**, *80*, 67–84; h) Y. S. Lee, R. S. Agnes, P. Davis, S.-W. Ma, H. Badghisi, J. Lai, F. Porreca, V. J. Hruby, *J. Med. Chem.* **2007**, *50*, 165–168.

[9] L. Gentilucci, G. Cardillo, A. Tolomelli, S. Spampinato, A. Spartà, F. Squassabia, *Eur. J. Org. Chem.* **2008**, 729–735.

[10] a) D. Lucet, T. Le Gall, C. Mioskowski, *Angew. Chem.* **1998**, *110*, 2724–2772; *Angew. Chem. Int. Ed.* **1998**, *37*, 2580–2627; b) V. Fedi, M. Altamura, G. Balacco, F. Canfarini, M. Criscuoli, D. Giannotti, A. Giolitti, S. Giuliani, A. Guidi, N. J. S. Harmat, R. Nannicini, F. Pasqui, R. Patacchini, E. Perrotta, M. Tramontana, A. Triolo, C. A. Maggi, *J. Med. Chem.* **2004**, *47*, 6935–6947.

[11] a) H. Sajiki, K. Y. Ong, *Tetrahedron* **1996**, *52*, 14507–14514.

[12] T. Morie, S. Kato, H. Harada, I. Fujiwara, K. Watanabe, J.-I. Matsumoto, *J. Chem. Soc. Perkin Trans.* **1994**, *1*, 2565–2569.

[13] a) For a leading reference on the use of a cryoprotective [D_6]DMSO/H_2O mixture as a biomimetic medium, see: P. A. Temussi, D. Picone, G. Saviano, P. Amodeo, A. Motta, T. Tancredi, S. Salvadori, R. Tomatis, *Biopolymers* **1992**, *32*, 367–372; b) L. Gentilucci, A. Tolomelli, *Curr. Topics Med. Chem.* **2004**, *4*, 105–121, and references herein.

[14] C. Toniolo, *CRC Crit. Rev. Biochem.* **1980**, *9*, 1–44.

[15] W. D. Cornell, P. Cieplak, C. I. Bayly, I. R. Gould, K. M. Merz, D. M. Ferguson, D. C. Spellmeyer, T. Fox, J. W. Caldwell, P. A. Kollman, *J. Am. Chem. Soc.* **1995**, *117*, 5179–5197.

[16] R. Haubner, R. Gratias, B. Diefenbach, S. L. Goodman, A. Joczyk, H. Kessler, *J. Am. Chem. Soc.* **1996**, *118*, 7461–7472.

[17] a) J. D. Dunitz, J. Waser *J. Am. Chem. Soc.* **1972**, *94*, 5645–5650; b) H. Kessler, R. Gratias, G. Hessler, M. Gurrath, G. Muller, *Pure Appl. Chem.* **1996**, *68*, 1201–1205.

[18] G. P. Curley, H. Blum, M. J. Humphries, *Cell. Mol. Life Sci.* **1999**, *56*, 427–441.

[19] a) M. A. Dechantsreiter, E. Planker, B. Matha, E. Lohof, G. Holzemann, A. Jonczyk, S. L. Goodman, H. Kessler, *J. Med. Chem.* **1999**, *42*, 3033–3040; b) C. Henry, N. Moitessier, Y. Chapleur, *Mini-Rev. Med. Chem.* **2002**, *2*, 531–542; c) B. Cacciari, G. Spalluto, *Curr. Med. Chem.* **2005**, *12*, 51–70.
[20] J.-P. Xiong, T. Stehle, R. Zhang, A. Joachimiak, M. Frech, S. L. Goodman, M. Amin Arnaout, *Science* **2002**, *296*, 151–155.
[21] L. Marinelli, A. Lavecchia, K.-E. Gottschalk, E. Novellino, H. Kessler, *J. Med. Chem.* **2003**, *46*, 4393–4404.
[22] M. Gurrath, G. Muller, H. Kessler, M. Aumailley, R. Timpl, *Eur. J. Biochem.* **1992**, *210*, 911–921.
[23] a) S. Caltabiano, W. T. Hum, G. J. Attwell, D. N. Gralnick, L. J. Budman, A. M. Cannistraci, F. Bex, *J. Biochem. Pharm.* **1999**, *58*, 1567–1578; b) H. Fujii, H. Komazawa, H. Mori, M. Kojima, I. Itoh, J. Murata, I. Azuma, I. Saiki, *Biol. Pharm. Bull.* **1995**, *18*, 1681–1688.
[24] M. S. Goligorsky, G. F. Dibona, *Proc. Natl. Acad. Sci. USA* **1993**, *90*, 5700–5704.
[25] VT-^{1}H NMR analysis of **10** is consistent with the secondary structure expected on the basis of the parent model **2**; $\Delta\delta/\Delta T$ (ppb K^{-1}): AspNH, −6.0; ArgNH, −5.0; NH^a, −4.2; NH^b, −1.0.
[26] *cyclo*-[RGDf(NMe)V] (Cilengitide, EMD 121974) inhibits the adhesion of fibronectin and other extracellular matrix proteins to various kinds of $\alpha_v\beta_3$-integrin-expressing cell lines at micromolar concentrations; for selected examples, see: a) T. Taga, A. Suzuki, I. Gonzalez-Gomez, F. H. Gilles, M. Stins, H. Shimada, L. Barsky, K. I. Weinberg, W. E. Laug, *Int. J. Cancer* **2002**, *98*, 690–697; b) L. Belvisi, T. Riccioni, M. Marcellini, L. Vesci, I. Chiarucci, D. Efrati, D. Potenza, C. Scolastico, L. Manzoni, K. Lombardo, M. A. Stasi, A. Orlandi, A. Ciucci, B. Nico, D. Ribatti, G. Giannini, M. Presta, P. Carminati, C. Pisano, *Mol. Cancer Ther.* **2005**, *4*, 1670–1680; c) S. Loges, M. Butzal, J. Otten, M. Schweizer, U. Fischer, C. Bokemeyer, D. K. Hossfeld, G. Schuch, W. Fiedler, *Biochem. Biophys. Res. Commun.* **2007**, *357*, 1016–1020, and references therein.
[27] W. L. Jorgensen, J. Chandrasekhar, J. Madura, R. W. Impey, M. L. Klein, *J. Chem. Phys.* **1983**, *79*, 926–935.
[28] H. J. C. Berendsen, J. P. M. Postma, W. F. van Gunsteren, A. DiNola, J. R. Haak, *J. Chem. Phys.* **1984**, *81*, 3684–3690.
[29] H. Shibata, T. Yagi, *Clin. Chim. Acta* **1996**, *251*, 53–64.

Received: November 24, 2008
Revised: January 28, 2009
Published online on February 18, 2009

